Hindawi
Mathematical Problems in Engineering
Volume 2019, Article ID 2491850, 16 pages
https://doi.org/10.1155/2019/2491850

Research Article

Secure Communications Based on the Projective Synchronization of Four-Dimensional Hyperchaotic Systems

Salahuddin Abdul Rahman,[1] Mohamed Zribi ,[1] and Nejib Smaoui [2]

[1]*Department of Electrical Engineering, Kuwait University, P.O. Box 5969, Safat 13060, Kuwait*
[2]*Department of Mathematics, Kuwait University, P.O. Box 5969, Safat 13060, Kuwait*

Correspondence should be addressed to Mohamed Zribi; mohamed.zribi10@gmail.com

Received 18 October 2018; Revised 23 April 2019; Accepted 19 May 2019; Published 30 May 2019

Academic Editor: Marcelo A. Savi

This paper deals with the projective synchronization (PS) of two identical discrete-time generalized four-dimensional (4D) hyperchaotic Henon maps using a master-slave configuration. A discrete sliding mode controller (DSMC) scheme is proposed to synchronize the master and the slave systems. The performance of the controlled systems is simulated; the simulation results indicate that the proposed controller works well. In addition, a secure communication scheme is proposed based on the developed control scheme. The validity of the proposed scheme is tested by transmitting an image and simulating the results. The simulation results clearly indicate the effectiveness of the proposed secure communication scheme.

1. Introduction

Chaos synchronization refers to the process wherein two or more chaotic systems adjust a given property of their motion to a common behavior by either coupling or forcing [1]. Depending upon the particular coupling configuration, the process leading to synchronized states is divided into two cases. These two cases are unidirectional coupling and bidirectional coupling. For the case of bidirectional coupling, both subsystems are coupled with each other. The coupling factor induces an adjustment of the rhythms onto a common synchronized manifold. As a result, a mutual synchronization behavior will be induced. This situation appears in nonlinear optics such as lasers [2], in physiology [3] or between interacting neurons [4].

On the other hand, the unidirectional coupling case is totally different from the bidirectional situation. In the unidirectional coupling, two subsystems form a global system using a drive-response (master-slave) configuration. The response system evolution will be driven by the drive system. Thus, the response system will be forced to follow the dynamics of the drive system and hence the latter will act as an external chaotic forcing of the response. The master-slave configuration of chaos has many applications in real life such as telecommunications [5], energy resource systems [6], electrical drives [7], gyro systems [8], satellites [9], and chaos authentication [10]. In 1990, ott et al. [11] were able to control chaos by forcing a chaotic system to follow a desired behavior; this control strategy is known as OGY method. In the same year, Peccora and Caroll [12] were able to control chaos through the method of chaos synchronization. After that, various schemes were successfully applied to chaos and hyperchaos synchronization for both continuous-time systems [13–21] and discrete-time systems [22–29].

The most common types of synchronization in interacting chaotic systems include complete synchronization (CS) [1], phase and antiphase synchronization [30], lag synchronization (LS) [31], generalized synchronization (GS) [32], anticipating synchronization (AS) [33], projective synchronization (PS) [34], and Q-S synchronization [24].

Chaotic signals have special properties that satisfy the requirements for secure communication systems, such as

irregularity, aperiodicity, broadband, and unpredictability. Because of these properties, several communication schemes using chaos were proposed and extensively studied [35–37].

Several methods were proposed in the literature for designing chaotic communication systems. One proposed method is chaotic masking where the message is added to the states of the transmitter [38, 39]. In this case, synchronization is needed at the receiver end to extract the message by performing subtraction from the synchronized states of the receiver. Another proposed method is chaotic modulation [40]. In this method, the message is used to modulate one parameter of a chaotic system at the transmitter end; then the message is recovered at the receiver end through synchronization. Also, the method of chaotic shift keying was proposed for transmitting digital messages [5, 41]. Synchronization is used in this method to reconstruct the message at the receiver end. Other secure communication methods include the inverse system approach [42] and chaos control method [43]. In all the previously mentioned methods, the transmitter and the receiver are synchronized to be able to reconstruct the message at the receiver end. Hence, synchronization is important to regenerate the chaotic carrier signal and thus recover the transmitted message.

Nowadays using computers and DSP chips to implement controllers of discrete-time systems has become very common and simple. Hence, several researchers have designed and implemented discrete-time secure communication systems [44–46].

The design of chaos based secure communication schemes has been tackled by many researchers. Several communication schemes were proposed in the unidirectional configuration [36] and the bidirectional configuration [47] for continuous-time systems [36, 48] and for discrete-time systems [47], using chaos synchronization [36], hyperchaos synchronization [45], projective synchronization [47], and other types of synchronization [36]. However, several techniques can be combined to further enhance the security and to make it easier to implement the proposed schemes.

This paper presents a discrete time sliding mode control law for the projective synchronization problem of discrete-time hyperchaotic systems. The proposed control law is then used to design a secure communication scheme. Hyperchaotic systems contain more complex dynamical characteristics than chaotic systems since the attractor has more than one positive Lyaponuv exponent [49]. Therefore, using hyperchaos synchronization to design secure communication schemes can enhance security. The proposed sliding mode controller uses one control input and gives a robust control method for hyperchaos synchronization in the master-slave configuration. In addition, when using projective synchronization, the states of the master and the slave systems synchronize up to a scaling factor [34]. This scaling factor can be used as an additional enhancement to the security of the communication scheme. Therefore, a key contribution of this paper the combination of projective synchronization with hyperchaos to enhance the security of the proposed communication scheme. Hence, the proposed secure communication scheme has better security performance and it is easier to implement.

The paper is organized as follows. The 4D hyperchaotic Henon map is described in Section 2. Section 3 presents the synchronization problem of two 4D hyperchaotic Henon maps using a discrete sliding mode controller; simulation results are presented. A secure communication using the synchronization of the 4D hyperchaotic Henon maps is developed in Section 4. Finally, some concluding remarks are given in Section 5.

2. The 4D Hyperchaotic Henon Map

2.1. Description of the 4D Hyperchaotic Henon Map. The discrete-time generalized four-dimensional hyperchaotic Henon map is described by a fourth order system of difference equations such as [50]

$$\begin{aligned} x_1(k+1) &= a - x_3^2(k) - bx_4(k) \\ x_2(k+1) &= x_1(k) \\ x_3(k+1) &= x_2(k) \\ x_4(k+1) &= x_3(k) \end{aligned} \tag{1}$$

where $x_1(k)$, $x_2(k)$, $x_3(k)$, and $x_4(k)$ are the state variables of the system and a, b are the parameters of the system. The system given by (1) exhibits chaotic behavior for $a = 1.767$ and $b = 0.1$. The plots of the state trajectories of the 4D hyperchaotic Henon map are shown in Figure 1.

The method described in the work of Geist et al. [51] is used to calculate the Lyapunov exponents for the 4D Henon map. The calculation was performed by running the system given by (1) for 100000 iterations. The Lyapunov exponents were found to be

$$\begin{aligned} \lambda_1 &= 0.1540, \\ \lambda_2 &= 0.1415, \\ \lambda_3 &= 0.1204, \\ \lambda_4 &= -2.7184 \end{aligned} \tag{2}$$

Since there exists three positive Lyapunov exponents, then the 4D Henon map is a hyperchaotic system [52].

This paper deals with the synchronization of two 4D huper-chaotic Henon maps using a master-slave configuration. Therefore, the following sub-section presents the model of the error system.

2.2. Model of the Error System. Let the master system be defined as the 4D Henon hyperchaotic map as follows:

$$\begin{aligned} x_1(k+1) &= a - x_3^2(k) - bx_4(k) \\ x_2(k+1) &= x_1(k) \\ x_3(k+1) &= x_2(k) \\ x_4(k+1) &= x_3(k) \end{aligned} \tag{3}$$

where $x_1(k), x_2(k), x_3(k)$, and $x_4(k)$ are the state variables of the master system and a, b are the parameters of the system.

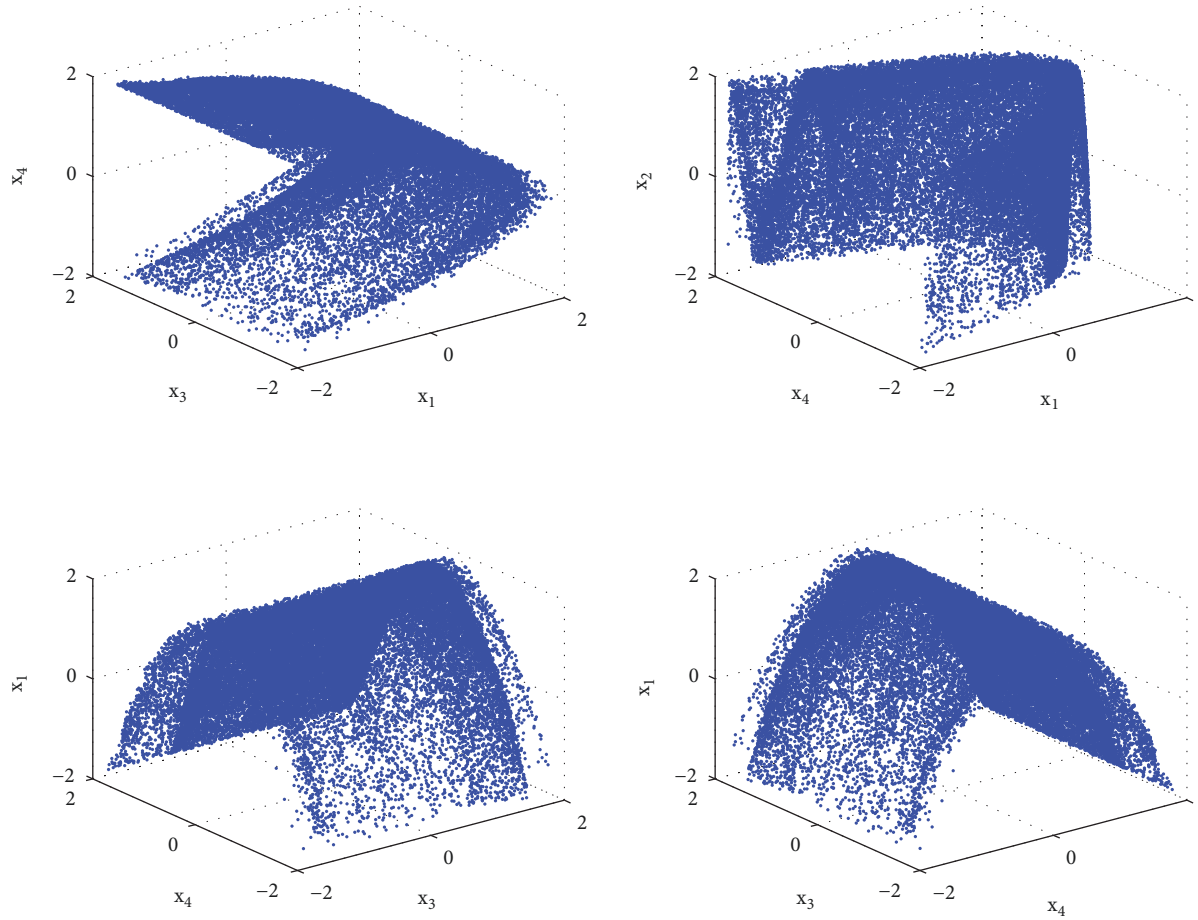

Figure 1: Plots of the state trajectories of the 4D hyperchaotic Henon map.

The slave system is defined as the 4D Henon hyperchaotic map as follows:

$$\begin{aligned} y_1(k+1) &= a - y_3^2(k) - by_4(k) + u(k) \\ y_2(k+1) &= y_1(k) \\ y_3(k+1) &= y_2(k) \\ y_4(k+1) &= y_3(k) \end{aligned} \tag{4}$$

where $y_1(k)$, $y_2(k)$, $y_3(k)$, and $y_4(k)$ are the state variables of the slave system. Note that a controller for the system which is represented by $u(k)$ is added to the first difference equation of the slave system. This controller will be designed for the purpose of the projective synchronization of the master and slave systems; i.e., $\lim_{k\longrightarrow\infty}|y(k) - \alpha x(k)| = 0$, where α is a design parameter.

Define the vectors $x(k)$ and $y(k)$ such that

$$x(k) = \left[x_1(k) \;\; x_2(k) \;\; x_3(k) \;\; x_4(k)\right]^T, \tag{5}$$

and

$$y(k) = \left[y_1(k) \;\; y_2(k) \;\; y_3(k) \;\; y_4(k)\right]^T. \tag{6}$$

Also, define the error $e(k)$ as follows:

$$e(k) = \left[e_1(k) \;\; e_2(k) \;\; e_3(k) \;\; e_4(k)\right]^T \tag{7}$$

where

$$e(k) = y(k) - \alpha x(k). \tag{8}$$

Using (3) and (4), the error dynamics can be written as follows:

$$\begin{aligned} e_1(k+1) &= (1-\alpha)a + \alpha x_3^2(k) - y_3^2(k) - be_4(k) \\ &\quad + u(k) \\ e_2(k+1) &= e_1(k) \\ e_3(k+1) &= e_2(k) \\ e_4(k+1) &= e_3(k). \end{aligned} \tag{9}$$

The objective of this paper is to synchronize the master and the slave system by forcing the state vector $y(k)$ of the slave system (4) to track the scaled state vector $\alpha x(k)$ of the master system (3); i.e., $\lim_{k\longrightarrow\infty} e(k) = \lim_{k\longrightarrow\infty} y(k) - \alpha x(k) = 0$. This is done by forcing the error $e(k)$ to converge to $(0, 0, 0, 0)$ as $k \longrightarrow \infty$. A sliding mode controller will be used for this purpose. The design of this controller will be discussed in the next section.

3. Synchronization of Two 4D Hyper-Chaotic Henon Maps Using a Sliding Mode Controller

3.1. Design of the Controller. The first step in the design of a sliding mode controller involves choosing the sliding surface. Since there is one control input in the slave system, then we need to choose one sliding surface.

Let c_1, c_2, and c_3 be design parameters such that the roots of the polynomial $P_2(s) = s^3 + c_1 s^2 + c_2 s + c_3 = 0$ are located inside the unit circle. The sliding surface $S(k)$ is chosen such that

$$S(k) = e_1(k) + c_1 e_2(k) + c_2 e_3(k) + c_3 e_4(k) \tag{10}$$

Also, define the sign function such that

$$\operatorname{sgn}(\sigma) = \begin{cases} 1 & \text{if } \sigma > 0 \\ 0 & \text{if } \sigma = 0 \\ -1 & \text{if } \sigma < 0. \end{cases} \tag{11}$$

The subsequent development requires that we define the concepts of quasi-sliding mode (QSM) and the quasi-sliding mode band (QSMB). These concepts were defined in [53]. The definitions are based on the following three attributes that the desired state trajectory of a discrete variable structure (VSC) system should have the following:

Attribute 1 (A1): starting from any initial state, the trajectory will move monotonically toward the switching plane and cross it in finite time.

Attribute 2 (A2): once the trajectory has crossed the switching plane for the first time, it will cross the plane in every successive sampling period, resulting in a zigzag motion about the switching plane.

Attribute 3 (A3): the size of each successive zigzagging step is nonincreasing and the trajectory stays within a specified band.

Definition 1 (see [53]). The motion of a discrete VSC system satisfying attributes A2 and A3 is called quasi-sliding mode (QSM). The specified band width contains the QSM is called the quasi-sliding mode band (QSMB) and it is as follows:

$$\{x \mid -\Delta < S(x) < \Delta\} \tag{12}$$

where 2Δ is the width of the band.

Let the control parameters be such that $T > 0$, $\epsilon_1 > 0$, $\epsilon_2 > 0$, $q > 0$, $1 - qT > 0$, $0 < \beta < 1$, and $\gamma > 1$.

The following theorem gives the main result of the paper.

Theorem 2. *The sliding mode controller,*

$$\begin{aligned} u(k) = {} & (1 - qT) S(k) - \epsilon_1 T |S(k)|^{\beta} \operatorname{sgn}(S(k)) \\ & - \epsilon_2 T |S(k)|^{\gamma} \operatorname{sgn}(S(k)) - c_1 e_1(k) - c_2 e_2(k) \\ & - c_3 e_3(k) + b e_4(k) - \alpha x_3^2(k) + y_3^2(k) - a \\ & + \alpha a, \end{aligned} \tag{13}$$

when applied to error system (9) guarantees the convergence of the errors to zero as $k \longrightarrow \infty$.

Proof. Using the sliding surface given by (10) and using the dynamic model of the errors (9) and the control law given by (13), we obtain

$$\begin{aligned} S(k+1) &= e_1(k+1) + c_1 e_2(k+1) + c_2 e_3(k+1) \\ &\quad + c_3 e_4(k+1) \\ &= a - \alpha a + \alpha x_3^2(k) - y_3^2(k) - b e_4(k) + u(k) \\ &\quad + c_1 e_1(k) + c_2 e_2(k) + c_3 e_3(k) \\ &= (1 - qT) S(k) - \epsilon_1 T |S(k)|^{\beta} \operatorname{sgn}(S(k)) \\ &\quad - \epsilon_2 T |S(k)|^{\gamma} \operatorname{sgn}(S(k)) \end{aligned} \tag{14}$$

Equation (14) corresponds to the double power reaching law defined in [54]. Note that (14) satisfies the reaching and existence condition given by $|S(k+1)| < |S(k)|$ which can be decomposed into the following two inequalities:

$$(S(k+1) - S(k)) \operatorname{sgn}(S(k)) < 0, \tag{15}$$

$$(S(k+1) + S(k)) \operatorname{sgn}(S(k)) \geq 0. \tag{16}$$

The above two inequalities can be proven as follows:

$$\begin{aligned} & (S(k+1) - S(k)) \operatorname{sgn}(S(k)) \\ & = \left(-qTS(k) - \epsilon_1 T |S(k)|^{\beta} \operatorname{sgn}(S(k))\right) \operatorname{sgn}(S(k)) \\ & \quad - \epsilon_2 T |S(k)|^{\gamma} \operatorname{sgn}(S(k)) \operatorname{sgn}(S(k)) \\ & = -qT |S(k)| - \epsilon_1 T |S(k)|^{\beta} - \epsilon_2 T |S(k)|^{\gamma} < 0. \end{aligned} \tag{17}$$

And,

$$\begin{aligned} & (S(k+1) + S(k)) \operatorname{sgn}(S(k)) \\ & = \left((2 - qT) S(k) - \epsilon_1 T |s(k)|^{\beta} \operatorname{sgn}(S(k))\right) \operatorname{sgn}(S(k) \\ & \quad - \epsilon_2 T |S(k)|^{\gamma} \operatorname{sgn}(S(k)) \operatorname{sgn}(S(k) \\ & = (2 - qT) |S(k)| - \epsilon_1 T |S(k)|^{\beta} - \epsilon_2 T |S(k)|^{\gamma} \end{aligned} \tag{18}$$

Since $(2 - qT) > 0$ and $|S(k)| > (1/(2 - qT))(\epsilon_1 T |S(k)|^{\beta} + \epsilon_2 T |S(k)|^{\gamma})$, then $(S(k+1) + S(k))\operatorname{sgn}(S(k)) > 0$.

Using inequalities (17) and (18), it follows that (14) satisfies the condition $|S(k+1)| < |S(k)|$ outside the QSMB. Hence, it can be concluded that $S(k)$ reaches zero in finite time.

On the sliding surface, $S(k) = 0$, we have

$$e_1(k) = -c_1 e_2(k) - c_2 e_3(k) - c_3 e_4(k) \tag{19}$$

Define the error $e_r(k)$ such that

$$e_r(k) = \begin{bmatrix} e_2(k) & e_3(k) & e_4(k) \end{bmatrix}^T. \tag{20}$$

Equations (9) and (19) allow us to obtain the following reduced order linear system:

$$e_r(k+1) = A_r e_r(k) \tag{21}$$

where

$$A_r = \begin{bmatrix} -c_1 & -c_2 & -c_3 \\ 1 & 0 & 0 \\ 0 & 1 & 0 \end{bmatrix}. \quad (22)$$

Since the control parameters c_1, c_2, c_3, and c_4 are chosen such that the matrix A_r is stable (i.e., the eigenvalues of A_r are inside the unit circle), then the errors $e_2(k)$, $e_3(k)$, and $e_4(k)$ converge to zero as $k \longrightarrow \infty$. Using (19), it can be concluded that the error $e_1(k)$ will also converge to zero as $k \longrightarrow \infty$. Therefore, the errors $e_1(k)$, $e_2(k)$, $e_3(k)$, and $e_4(k)$ converge to zero as $k \longrightarrow \infty$. □

The convergence of the errors $e_1(k)$, $e_2(k)$, e_3(k), and $e_4(k)$ to zero as $k \longrightarrow \infty$ guarantees that $y_1(k)$, $y_2(k)$, $y_3(k)$, and $y_4(k)$ converge to $\alpha x_1(k)$, $\alpha x_2(k)$, $\alpha x_3(k)$, and $\alpha x_4(k)$, respectively, as $k \longrightarrow \infty$. Hence, the states of the master and the slave hyper-chaotic systems are synchronized.

3.2. Simulation Results. The sliding mode controller given by (13) is applied to the hyperchaotic 4D Henon-maps given by (3) and (4). The MATLAB software is used to simulate the performances of the controlled systems. To obtain the hyperchaotic behavior of the 4D hyperchaotic Henon map, the parameters a and b are taken to be 1.76 and 0.1, respectively. The initial conditions of the master system (3) are taken to be $x_1(0) = 0.1$, $x_2(0) = -0.1$, $x_3(0) = 0.1$, and $x_4(0) = 0.1$. On the other hand, the initial conditions of the slave system (4) are taken to be $y_1(0) = -0.2$, $y_2(0) = 0.2$, $y_3(0) = -0.2$, and $y_4(0) = 0.2$. The projective synchronization factor is $\alpha = -2$. The parameters of the controller are chosen such that $T = 1$, $\epsilon_1 = 0.1$, $\epsilon_2 = 0.1$, $q = 0.9$, $\alpha = 0.8$, $\gamma = 1.2$, $\delta = 0.002$, $c_1 = 0.01$, $c_2 = 0$, and $c_3 = 0$. The performance of the system is simulated from $k = 0$ till $k = 100$. For $k < 50$, the performance of the system is simulated with $u = 0$. Then, for $k \geq 50$ the controller u is applied to the slave system. In addition, to avoid the occurrence of chattering, the saturation function is used to replace the discontinuous sign function in the control law such that $sat(S) = S/(|S| + \delta)$, where δ is a small positive scalar which can be chosen to get a very good approximation.

The simulation results are presented in Figures 2–11. The plots of the states of the hyperchaotic 4D Henon maps versus k are depicted in Figures 2–5. The plots of the errors versus k are shown in Figures 6–10. The controller versus k is shown in Figure 10. Also, the strange attractors of the master and slave systems are shown in Figure 11.

Figures 2–5 clearly show that the two hyperchaotic Henon maps are synchronized after the application of the proposed sliding mode controller. Figures 6–9 indicate that the errors for the hyper-chaotic 4D Henon maps converge to zero as k tends to infinity. Hence, the simulation results show that the proposed sliding mode controller works well as it is able to synchronize the master and the slave systems.

To show the effects of using the saturation function instead of the sign function in the controller, we present the error e_1 versus k when using the sign function (Figure 12) and the error e_1 versus k when using the saturation function (Figure 13). It can be seen from these two figures that the usage of the saturation function has greatly reduced the chattering.

3.3. Robustness of the Proposed Controller. To study the robustness of the proposed controller, we will assume that there is a mismatch between the parameters a and b of the 4D hyperchaotic Henon maps and the parameters a and b of the controller. We will denote the parameters a and b of the controller as $\overline{a}$ and $\overline{b}$ such that $\overline{a} = a + \Delta a$ and $\overline{b} = b + \Delta b$.

Using the parameters $\overline{a}$ and $\overline{b}$, the sliding mode controller (13) becomes

$$\begin{aligned} u(k) = {} & (1 - qT) S(k) - \epsilon_1 T |S(k)|^{\beta} \operatorname{sgn}(S(k)) \\ & - \epsilon_2 T |S(k)|^{\gamma} \operatorname{sgn}(S(k)) - c_1 e_1(k) - c_2 e_2(k) \\ & - c_3 e_3(k) + \overline{b} e_4(k) - \alpha x_3^2(k) + y_3^2(k) - \overline{a} \\ & + \alpha \overline{a} \end{aligned} \quad (23)$$

The sliding mode controller given by (23) is applied to the chaotic Henon maps given by (3) and (4) for different values of Δa and Δb. The initial conditions and the other parameters of the controller are the same as in the previous subsection.

Figure 14 depicts the errors $e_1(k)$, $e_2(k)$, $e_3(k)$, and $e_4(k)$ versus k when using the sliding mode controller and with $\Delta a = -0.01$ and $\Delta b = 0.2$ (case 1). Figure 15 shows the errors $e_1(k)$, $e_2(k)$, $e_3(k)$, and $e_4(k)$ versus k when using the sliding mode controller and with $\Delta a = 0.04$ and $\Delta b = 0.75$ (case 2).

Therefore, Figures 14-15 indicate that the proposed controller works well when there is a mismatch between the parameters of the controller and those of the 4D hyperchaotic Henon maps. Thus, it can be concluded that the simulation studies indicate that the developed sliding mode control scheme is robust with respect to mismatches between the parameters of the controller and those of the the 4D hyperchaotic Henon maps.

4. A Secure Communication Scheme Using the 4D Hyperchaotic Maps

4.1. Overview of the Secure Communication Scheme. In this section, the previously proposed approach of synchronization is used to implement a secure communication scheme. The chaotic masking method, where the message signal is added to a chaotic carrier, will be used. A block diagram depiction of the communication scheme is presented in Figure 16.

The different steps involved in the chaotic masking method are the following.

(1) At the transmitter side, the master system is represented by a system of difference equations as follows:

$$x_m(k+1) = f\left(x_m(k)\right) \quad (24)$$

(2) The information message to be transmitted, $m(k)$, is added to the states of the master system $x_m(k)$ to obtain the masked signal

$$w_m(k) = C x_m(k) + \gamma m(k) \quad (25)$$

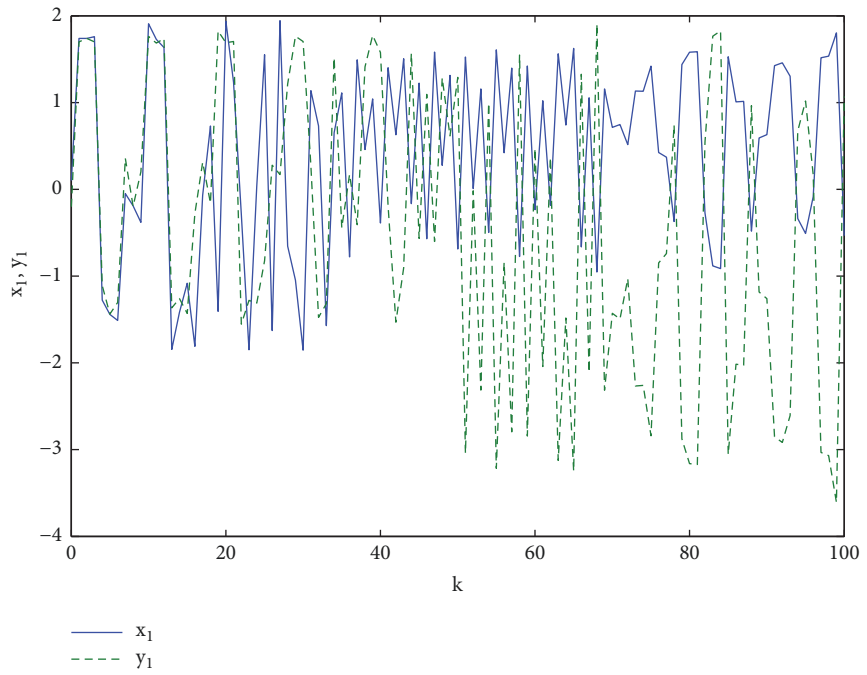

Figure 2: The states x_1 and y_1 versus k when using the sliding mode controller to synchronize the hyperchaotic systems.

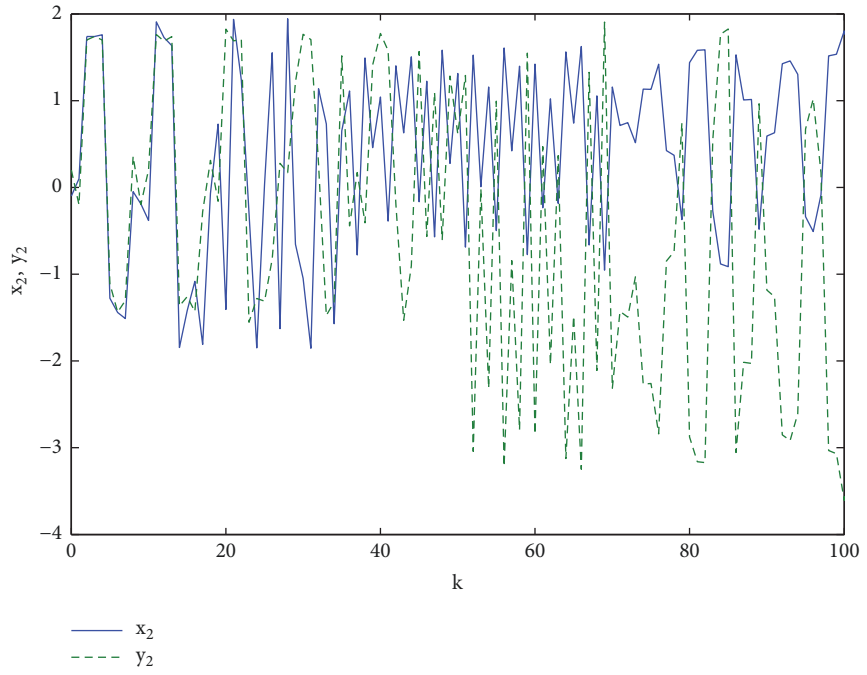

Figure 3: The states x_2 and y_2 versus k when using the sliding mode controller to synchronize the hyperchaotic systems.

where $x_m(k)$ is the state vector, C is an $m \times m$ matrix, and $\gamma = [\gamma_1, \gamma_2, \ldots \gamma_m]$ is a scaling vector.

(3) The masked signals $w_m(k)$ are multiplied by the projective synchronization factor α and then sent through a public channel.

(4) The public channel will add noise to the transmitted signals $\alpha w_m(k)$ and thus the signals are denoted by $\alpha \widetilde{w}_m(k)$.

(5) At the receiver side, the slave system is represented by the following system of difference equations:

$$y_m(k+1) = f\left(y_m(k), u(k)\right) \tag{26}$$

where $u(k)$ is the controller which will be used to synchronize the master and slave systems.

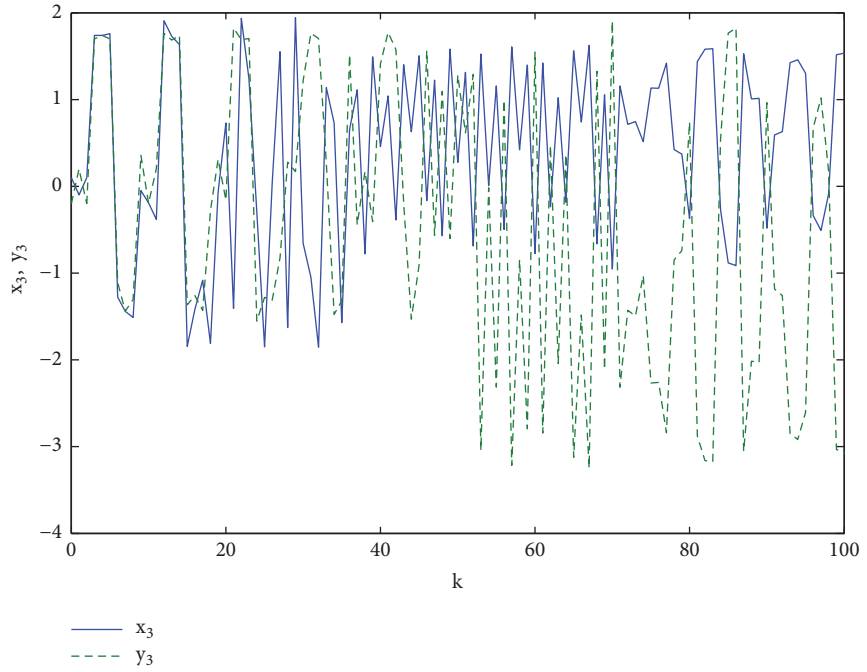

FIGURE 4: The states x_3 and y_3 versus k when using the sliding mode controller to synchronize the hyperchaotic systems.

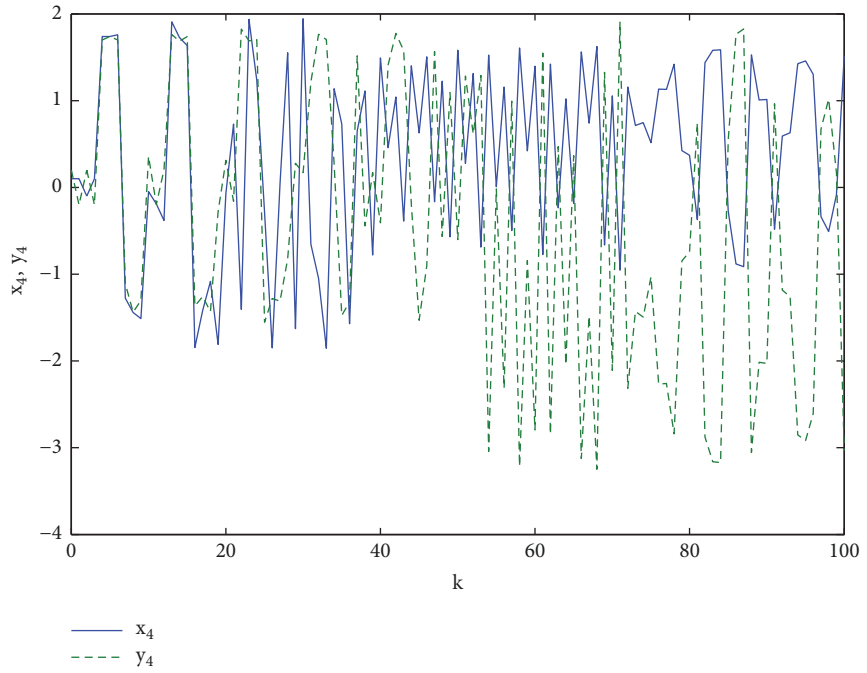

FIGURE 5: The states x_4 and y_4 versus k when using the sliding mode controller to synchronize the hyperchaotic systems.

(6) The previously proposed controller will then be used to synchronize the master and the slave systems. The error between the master and slave systems is defined as

$$\widetilde{e}(k) = y_m(k) - \alpha\widetilde{w}(k). \tag{27}$$

(7) To recover the information message, the states of the slave system $y_m(k)$ are subtracted from the states of the received signal $\widetilde{w}_m(k)$ and then one obtain the information signal corrupted with some additive noise due to the public channel. Hence we get

$$\eta\widetilde{m}(k) = \frac{1}{\alpha}\left(\alpha\widetilde{w}_m(k) - Cy_m(k)\right). \tag{28}$$

4.2. A Secure Communication Scheme Based on the 4D Hyper-Chaotic Henon Maps. The communication scheme is used

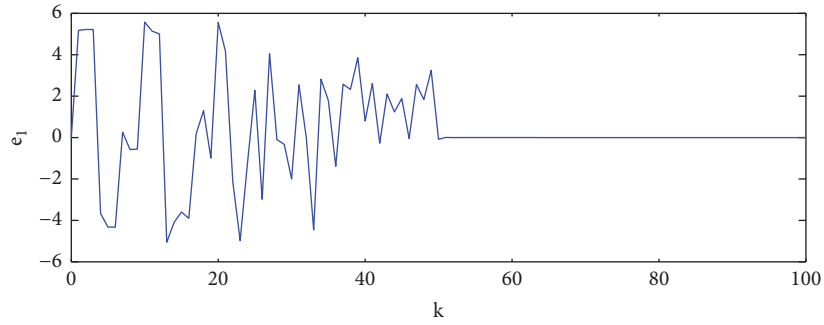

Figure 6: The error e_1 versus k when using the sliding mode controller to synchronize the hyperchaotic systems.

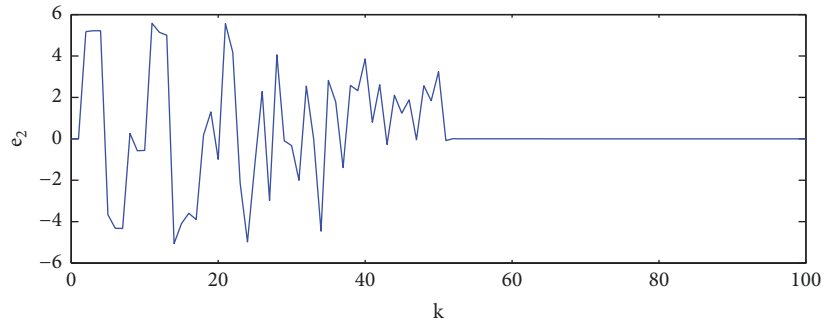

Figure 7: The error e_2 versus k when using the sliding mode controller to synchronize the hyperchaotic systems.

to send confidential information using 4D Henon maps as depicted in Figure 16. In this case, the master system is defined as the 4D hyperchaotic Henon map as follows:

$$\begin{aligned} x_1(k+1) &= a - x_3^2(k) - bx_4(k) \\ x_2(k+1) &= x_1(k) \\ x_3(k+1) &= x_2(k) \\ x_4(k+1) &= x_3(k) \end{aligned} \tag{29}$$

The matrix C in (25) is chosen to be

$$C = \begin{bmatrix} 1 & 0 & 0 & 0 \\ 0 & 1 & 0 & 0 \\ 0 & 0 & 1 & 0 \\ 0 & 0 & 0 & 1 \end{bmatrix} \tag{30}$$

and the scaling vector in (25) is such that $\eta = [\eta_1, 0, 0, 0]^T$, so that the information is added to the first state of the master system. The combined signal $w_m(k)$ is then sent through a public channel.

$$\begin{bmatrix} w_1(k) \\ w_2(k) \\ w_3(k) \\ w_4(k) \end{bmatrix} = \begin{bmatrix} x_1(k) + \eta_1 m(k) \\ x_2(k) \\ x_3(k) \\ x_4(k) \end{bmatrix}. \tag{31}$$

On the other hand, the slave system is defined as the 4D hyperchaotic Henon map as follows:

$$\begin{aligned} y_1(k+1) &= a - y_3^2(k) - by_4(k) + u(k) \\ y_2(k+1) &= y_1(k) \\ y_3(k+1) &= y_2(k) \\ y_4(k+1) &= y_3(k) \end{aligned} \tag{32}$$

Define the errors $\widetilde{e}_1(k)$, $\widetilde{e}_2(k)$, $\widetilde{e}_3(k)$, and $\widetilde{e}_4(k)$ such that

$$\begin{aligned} \widetilde{e}_1(k) &= y_1(k) - \alpha\widetilde{w}_1(k) \\ \widetilde{e}_2(k) &= y_2(k) - \alpha\widetilde{x}_2(k) \\ \widetilde{e}_3(k) &= y_3(k) - \alpha\widetilde{x}_3(k) \\ \widetilde{e}_4(k) &= y_4(k) - \alpha\widetilde{x}_4(k) \end{aligned} \tag{33}$$

where $\widetilde{w}_1(k)$, $\widetilde{x}_2(k)$, $\widetilde{x}_3(k)$, and $\widetilde{x}_4(k)$ are the transmitted signals corrupted with noise.

We will use the proposed sliding mode controller designed previously to synchronize the master and the slave 4D hyperchaotic Henon map.

Let the sliding surface $S(k)$ be such that

$$S(k) = \widetilde{e}_1 + c_1\widetilde{e}_2(k) + c_2\widetilde{e}_3(k) + c_3\widetilde{e}_4(k) \tag{34}$$

Using the results presented in Section 3, we will have the following proposition.

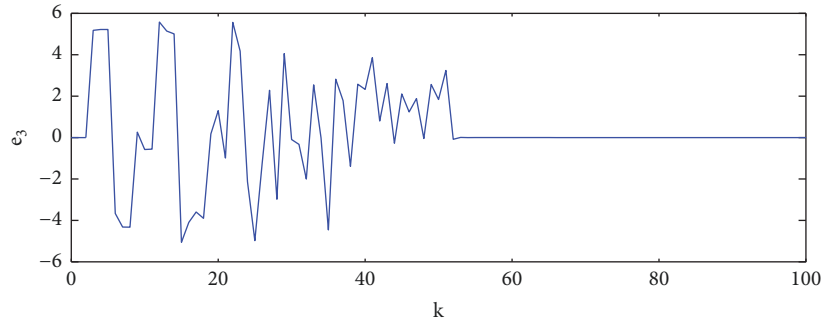

Figure 8: The error e_3 versus k when using the sliding mode controller to synchronize the hyperchaotic systems.

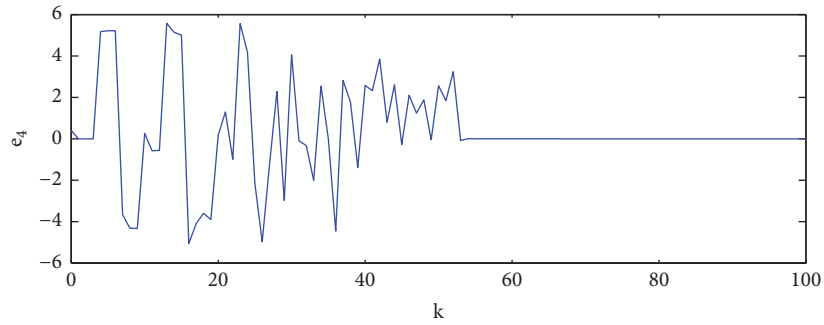

Figure 9: The error e_4 versus k when using the sliding mode controller to synchronize the hyperchaotic systems.

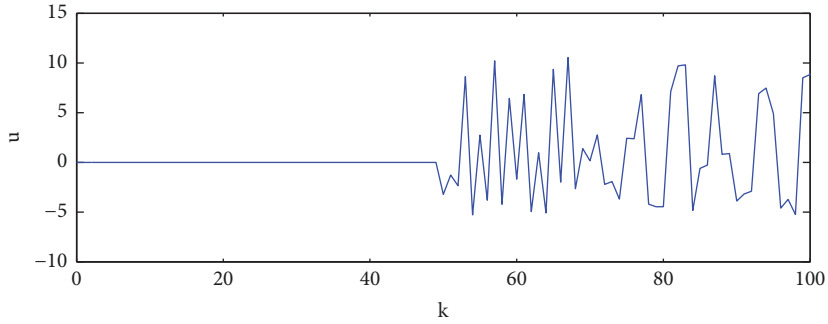

Figure 10: The sliding mode controller u versus k.

Proposition 3. *The following sliding mode controller*

$$\begin{aligned} u(k) = {} & (1 - qT) S(k) - \epsilon_1 T |S(k)|^{\beta} \operatorname{sgn}(S(k)) \\ & - \epsilon_2 T |S(k)|^{\gamma} \operatorname{sgn}(S(k)) - c_1 \widetilde{e}_1(k) - c_2 \widetilde{e}_2(k) \\ & - c_3 \widetilde{e}_3(k) + b \widetilde{e}_4(k) - \alpha \widetilde{x}_3^2(k) + y_3^2(k) - a \\ & + \alpha a \end{aligned} \tag{35}$$

where $\widetilde{e}_1(k)$, $\widetilde{e}_2(k)$, $\widetilde{e}_3(k)$, *and* $\widetilde{e}_4(k)$ *are given by (33) and* $T > 0$, $\epsilon_1 > 0$, $\epsilon_2 > 0$, $q > 0$, $1 - qT > 0$, $0 < \alpha < 1$, *and* $\gamma > 1$ *guarantee that the errors* $\widetilde{e}_1(k)$, $\widetilde{e}_2(k)$, $\widetilde{e}_3(k)$, *and* $\widetilde{e}_4(k)$ *converge to zero as* $k \longrightarrow \infty$.

The sliding mode controller given by (35) is applied to the systems given by (29) and (32). The MATLAB software is used to simulate the performances of the controlled systems. The initial conditions are taken as $x_1(0) = 0.1$, $x_2(0) = -0.1$, $x_3(0) = 0.1$, $x_4(0) = -0.1$ and $y_1(0) = -0.2$, $y_2(0) = 0.2$, $y_3(0) = -0.2$, $y_4(0) = -0.2$. The parameters of the controller are chosen such that $T = 1$, $\epsilon_1 = 0.1$, $\epsilon_2 = 0.1$, $q = 0.9$, $\alpha = 0.8$, $\gamma = 1.2$, $\delta = 0.002$, $c_1 = 0.01$, $c_2 = 0$, and $c_3 = 0$. The scaling factor $\gamma_1 = 0.001$. The projective synchronization factor is given by $\alpha = -2$. The transmitted information $m(k)$ is an RGB (red, green, and blue) image as shown in Figure 17.

The RGB image shown in Figure 17 is represented by an $M \times N \times P$ matrix with values M=225, N=225, P=3. This matrix is converted into a one-dimensional array which can be expressed as follows: $m_s = [m_1, m_2, m_3, \ldots\ldots, m_{151875}]$. The sequence m_s is converted into a discrete signal $m(k)$ and then added to the first state of the hyperchaotic master system.

Since the information will be transmitted through a public channel, an additive white Gaussian noise (AWGN) is added to the transmitted signal with a $40dB$ Signal-to-noise ratio (SNR). The simulations are presented in Figures 18–23. Figure 18 depicts the recovered image when using the sliding

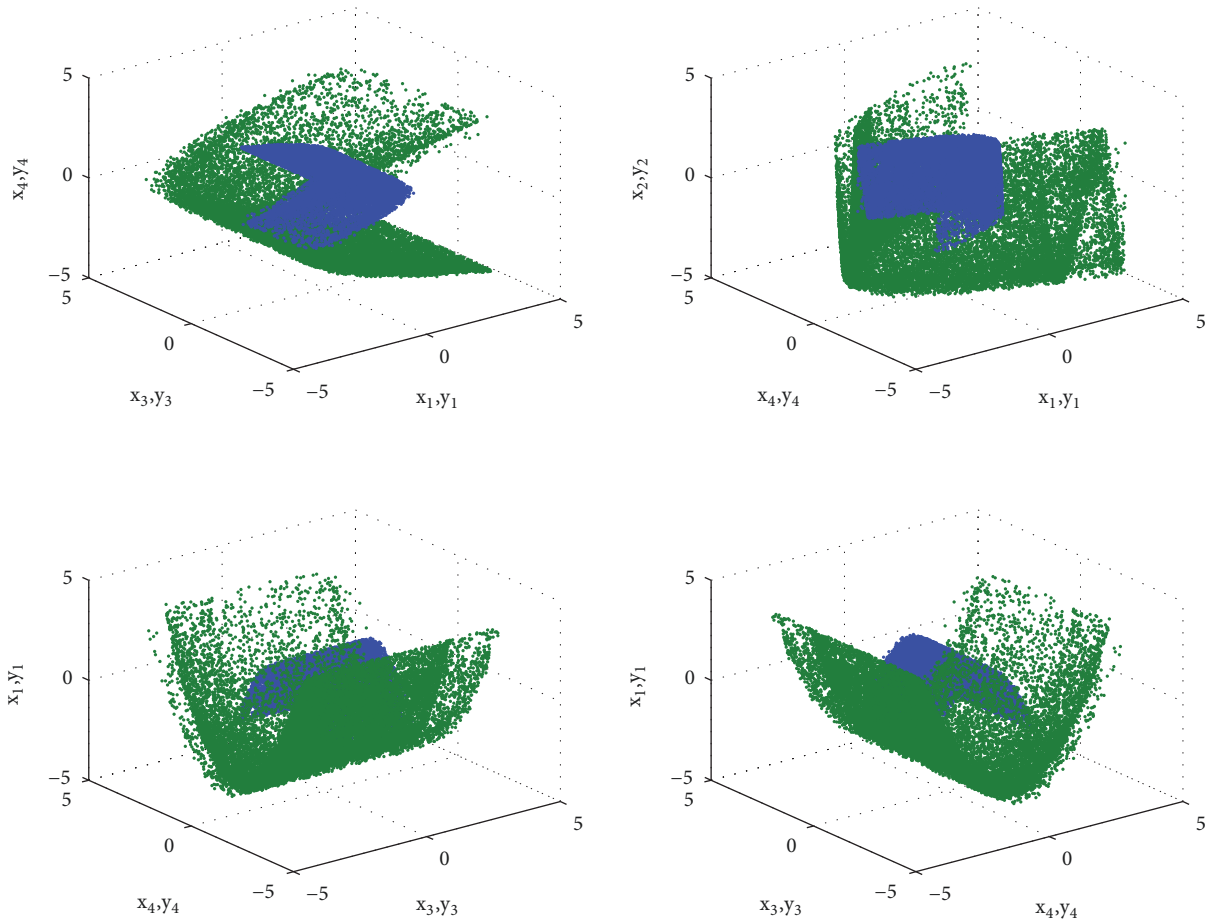

Figure 11: The strange attractors of the master and the slave systems when using the sliding mode controller.

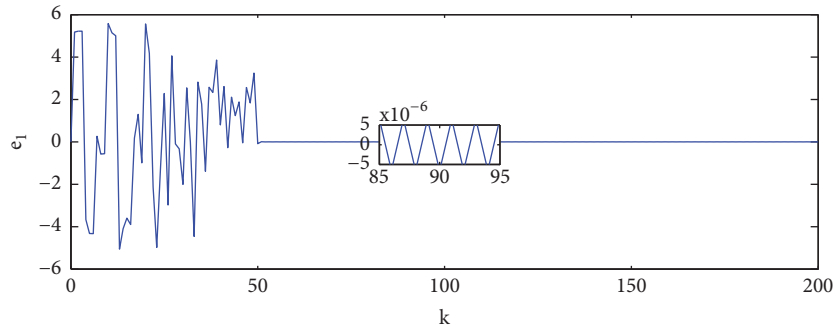

Figure 12: The error e_1 versus k when using the sign function in the sliding mode controller.

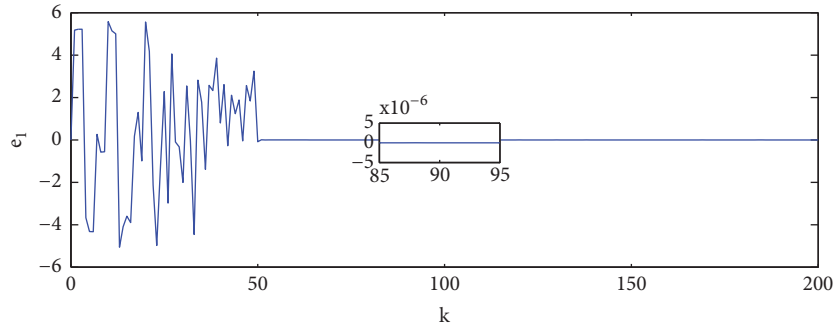

Figure 13: The error e_1 versus k when using the saturation function in the sliding mode controller.

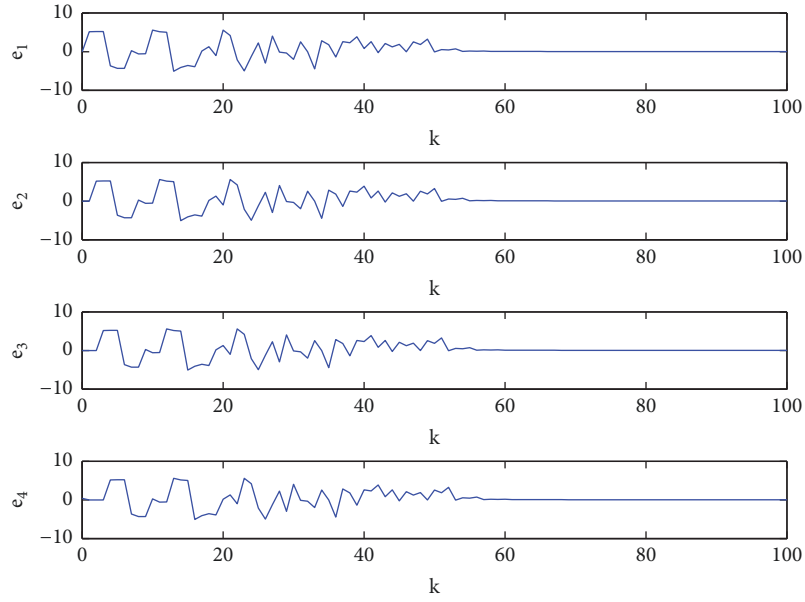

FIGURE 14: The errors e_1, e_2, e_3, and e_4 versus k when using the sliding mode controller and with mismatch in the parameters of the systems and the controller (case 1).

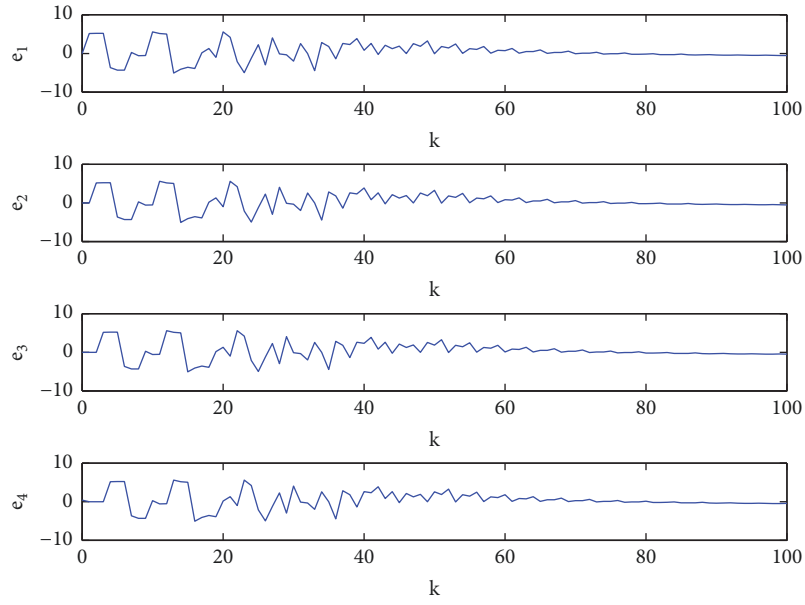

FIGURE 15: The errors e_1, e_2, e_3, and e_4 versus k when using the sliding mode controller and with mismatch in the parameters of the systems and the controller (case 2).

mode controller. Figure 19 shows the states $\widetilde{w}_1(k)$ and $y_1(k)$ versus k; the errors $\widetilde{e}_1$, $\widetilde{e}_2$, $\widetilde{e}_3$, and $\widetilde{e}_4$ versus k are shown in Figures 18–23, respectively.

Therefore, it is clear that the proposed communication scheme works well. Hence, it can be concluded that the projective synchronization of two 4D Henon maps can be used for secure communication purposes.

5. Conclusion

The projective synchronization problem is investigated for the hyperchaotic 4D Henon maps. A discrete sliding mode control scheme is proposed to achieve projective chaos synchronization by forcing the errors between the states of the master and the slave systems to converge to zero. The simulation results indicate that the proposed controller works well. Then, the proposed control scheme is used to design a secure communication scheme using 4D Henon maps synchronization. The proposed scheme is validated by transmitting an image through a public channel and recovering the sent image. The simulation results show that the proposed secure communication scheme works well.

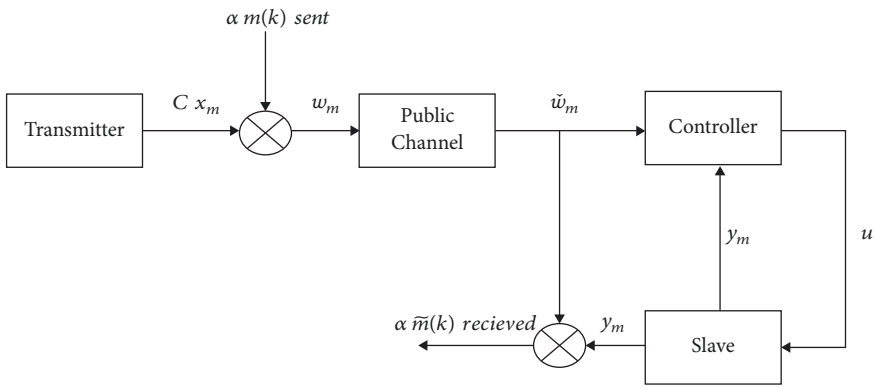

Figure 16: Block Diagram of the secure communication scheme.

Figure 17: The transmitted image.

Figure 18: The recovered image when using the sliding mode controller.

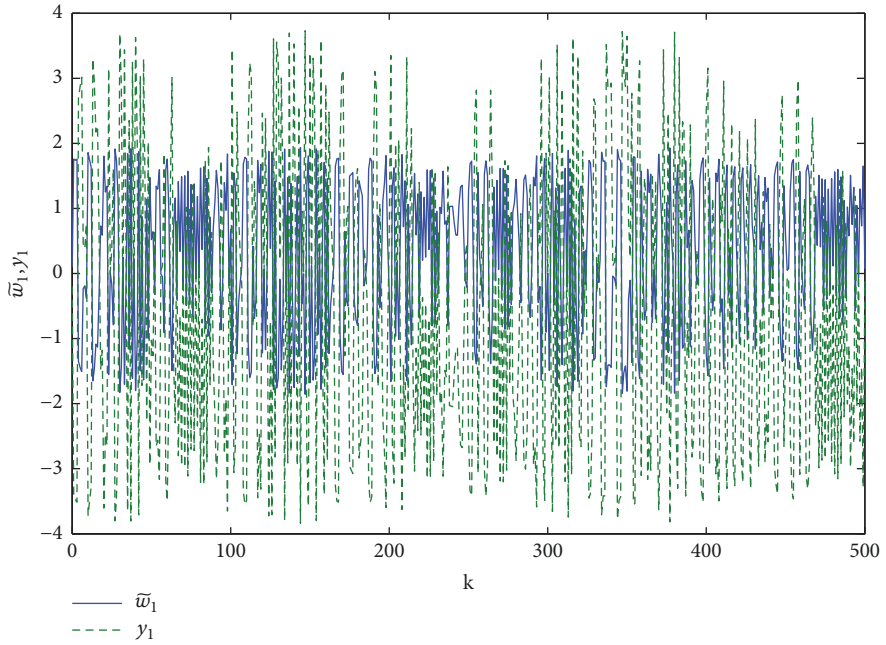

FIGURE 19: The states $\widetilde{w}_1(k)$ and $y_1(k)$ versus k when using the sliding mode controller.

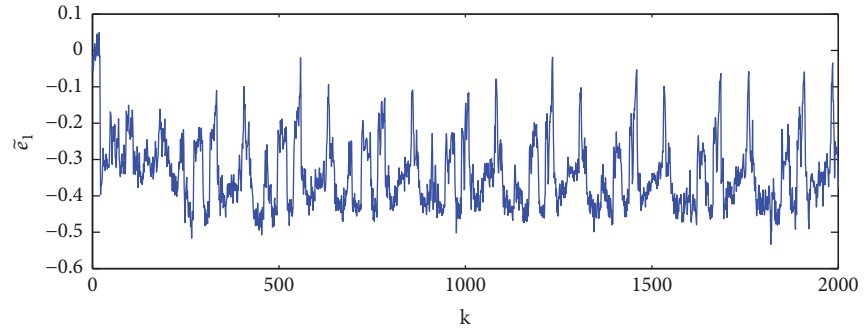

FIGURE 20: Part of the error $\widetilde{e}_1$ versus k when using the sliding mode controller.

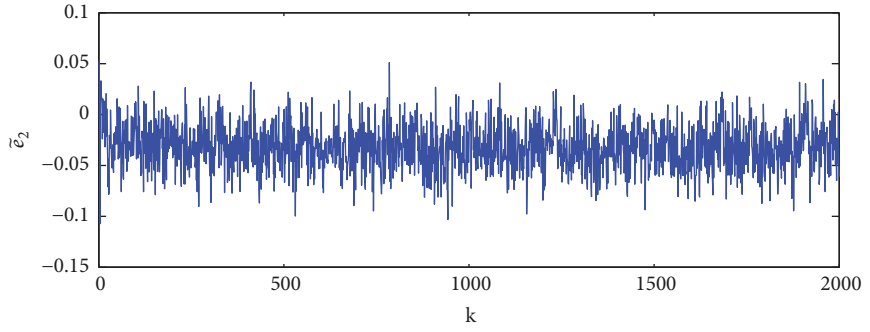

FIGURE 21: Part of the error $\widetilde{e}_2$ versus k when using the sliding mode controller.

Future work will address the usage of other nonlinear control techniques to synchronize discrete chaotic and hyperchaotic systems. Also, different methods to transmit information using discrete chaotic and hyperchaotic systems will be analyzed. Moreover, other transmission methods will be investigated to further enhance the security of communication schemes.

Data Availability

All the data was presented in the paper.

Conflicts of Interest

The authors declare that they have no conflicts of interest.

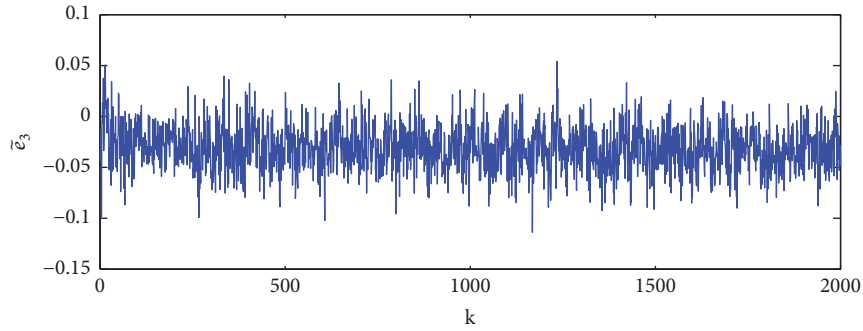

Figure 22: Part of the error $\tilde{e}_3$ versus k when using the sliding mode controller.

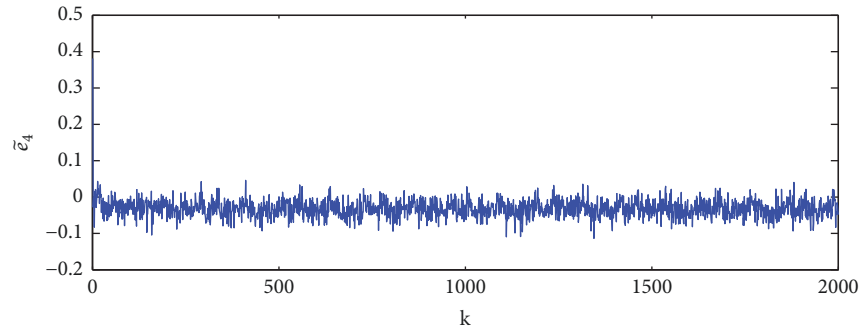

Figure 23: Part of the error $\tilde{e}_4$ versus k when using the sliding mode controller.

References

[1] S. Boccaletti, J. Kurths, G. Osipov, D. L. Valladares, and C. S. Zhou, "The synchronization of chaotic systems," *Physics Reports*, vol. 366, no. 1-2, pp. 1–101, 2002.

[2] R. Roy and K. S. Thornburg Jr., "Experimental synchronization of chaotic lasers," *Physical Review Letters*, vol. 72, no. 13, article 2009, 1994.

[3] L. Glass, "Synchronization and rhythmic processes in physiology," *Nature*, vol. 410, no. 6825, pp. 277–284, 2001.

[4] Q. Y. Wang, Q. S. Lu, G. R. Chen, and D. H. Guo, "Chaos synchronization of coupled neurons with gap junctions," *Physics Letters A*, vol. 356, no. 1, pp. 17–25, 2006.

[5] H. Dedieu, M. P. Kennedy, and M. Hasler, "Chaos shift keying: modulation and demodulation of a chaotic carrier using self-synchronizing Chua's circuits," *IEEE Transactions on Circuits and Systems II: Analog and Digital Signal Processing*, vol. 40, no. 10, pp. 634–642, 1993.

[6] Z. Wang, "Chaos synchronization of an energy resource system based on linear control," *Nonlinear Analysis: Real World Applications*, vol. 11, no. 5, pp. 3336–3343, 2010.

[7] Y. Sun, X. Wu, L. Bai, Z. Wei, and G. Sun, "Finite-time synchronization control and parameter identification of uncertain permanent magnet synchronous motor," *Neurocomputing*, vol. 207, pp. 511–518, 2015.

[8] H.-T. Yau, "Chaos synchronization of two uncertain chaotic nonlinear gyros using fuzzy sliding mode control," *Mechanical Systems and Signal Processing*, vol. 22, no. 2, pp. 408–418, 2008.

[9] S. M. Hamidzadeh and R. Esmaelzadeh, "Control and synchronization chaotic satellite using active control," *International Journal of Computer Applications*, vol. 94, no. 10, pp. 29–33, 2014.

[10] T.-L. Liao, P.-Y. Wan, P.-C. Chien, Y.-C. Liao, L.-K. Wang, and J.-J. Yan, "Design of high-security USB flash drives based on chaos authentication," *Electronics (Switzerland)*, vol. 7, no. 6, p. 82, 2018.

[11] E. Ott, C. Grebogi, and J. A. Yorke, "Controlling chaos," *Physical Review Letters*, vol. 64, no. 11, pp. 1196–1199, 1990.

[12] L. M. Pecora and T. L. Carroll, "Synchronization in chaotic systems," *Physical Review Letters*, vol. 64, no. 8, pp. 821–824, 1990.

[13] X. Zhang and H. Zhu, "Anti-synchronization of two different hyperchaotic systems via active and adaptive control," *International Journal of Nonlinear Science*, vol. 6, no. 3, pp. 216–223, 2008.

[14] C. Wang and S. S. Ge, "Adaptive synchronization of uncertain chaotic systems via backstepping design," *Chaos, Solitons & Fractals*, vol. 12, no. 7, pp. 1199–1206, 2001.

[15] H. Yau, "Design of adaptive sliding mode controller for chaos synchronization with uncertainties," *Chaos, Solitons & Fractals*, vol. 22, no. 2, pp. 341–347, 2004.

[16] G. Millerioux and J. Daafouz, "An observer-based approach for input-independent global chaos synchronization of discrete-time switched systems," *IEEE Transactions on Circuits and Systems I: Fundamental Theory and Applications*, vol. 50, no. 10, pp. 1270–1279, 2003.

[17] C.-K. Cheng and P. C.-P. Chao, "Chaos synchronization between Josephson junction and classical chaotic system via iterative learning control," in *Proceedings of the 4th IEEE International Conference on Applied System Innovation, ICASI 2018*, pp. 1232–1235, Japan, April 2018.

[18] M. M. El-Dessoky, E. O. Alzahrani, and N. A. Almohammadi, "Chaos control and function projective synchronization of

noval chaotic dynamical system," *Journal of Computational Analysis & Applications*, vol. 26, no. 1, 2019.

[19] Y. Batmani, "Chaos control and chaos synchronization using the state-dependent Riccati equation techniques," *Transactions of the Institute of Measurement and Control*, vol. 41, no. 2, pp. 311–320, 2018.

[20] D. Zhang, A. Zhao, X. Yang, Y. Sun, and J. Xiao, "Generalized synchronization between chen system and rucklidge system," *IEEE Access*, vol. 7, pp. 8519–8526, 2019.

[21] A. Hafiz, R. Héctor, and I. Salgado, "Robust synchronization of master slave chaotic systems: a continuous sliding-mode control approach with experimental study," in *Recent Advances in Chaotic Systems and Synchronization*, pp. 261–275, Academic Press, 2019.

[22] Y.-J. Xue and S.-Y. Yang, "Synchronization of generalized Henon map by using adaptive fuzzy controller," *Chaos, Solitons & Fractals*, vol. 17, no. 4, pp. 717–722, 2003.

[23] L. Huang, M. Wang, and R. Feng, "Synchronization of generalized Henon map via backstepping design," *Chaos, Solitons & Fractals*, vol. 23, no. 2, pp. 617–620, 2005.

[24] Z. Yan, "Q-S synchronization in 3D Hénon-like map and generalized Hénon map via a scalar controller," *Physics Letters A*, vol. 342, no. 4, pp. 309–317, 2005.

[25] G. Grassi and D. A. Miller, "Theory and experimental realization of observer-based discrete-time hyperchaos synchronization," *IEEE Transactions on Circuits and Systems I: Fundamental Theory and Applications*, vol. 49, no. 3, pp. 373–378, 2002.

[26] Z. Yan, "A nonlinear control scheme to anticipated and complete synchronization in discrete-time chaotic (hyperchaotic) systems," *Physics Letters A*, vol. 343, no. 6, pp. 423–431, 2005.

[27] T. Ushio, "Chaotic synchronization and controlling chaos based on contraction mappings," *Physics Letters A*, vol. 198, no. 1, pp. 14–22, 1995.

[28] X. Yin, Y. Ren, and X. Shan, "Synchronization of discrete spatiotemporal chaos by using variable structure control," *Chaos, Solitons & Fractals*, vol. 14, no. 7, pp. 1077–1082, 2002.

[29] A. Ouannas and Z. Odibat, "Generalized synchronization of different dimensional chaotic dynamical systems in discrete time," *Nonlinear Dynamics*, vol. 81, no. 1-2, pp. 765–771, 2015.

[30] M.-C. Ho, Y.-C. Hung, and C.-H. Chou, "Phase and anti-phase synchronization of two chaotic systems by using active control," *Physics Letters A*, vol. 296, no. 1, pp. 43–48, 2002.

[31] S. Taherion and Y.-C. Lai, "Observability of lag synchronization of coupled chaotic oscillators," *Physical Review E*, vol. 59, no. 6, pp. R6247–R6250, 1999.

[32] N. F. Rulkov, M. M. Sushchik, L. S. Tsimring, and H. D. I. Abarbanel, "Generalized synchronization of chaos in directionally coupled chaotic systems," *Physical Review E: Statistical, Nonlinear, and Soft Matter Physics*, vol. 51, no. 2, pp. 980–994, 1995.

[33] H. U. Voss, "Anticipating chaotic synchronization," *Physical Review E*, vol. 61, no. 5, pp. 5115–5119, 2000.

[34] R. Mainieri and J. Rehacek, "Projective synchronization in three-dimensional chaotic systems," *Physical Review Letters*, vol. 82, no. 15, pp. 3042–3045, 1999.

[35] T. Yang, "A survey of chaotic secure communication systems," *International Journal of Computational Cognition*, vol. 2, no. 2, pp. 81–130, 2004.

[36] B. Wang, X. Zhang, and X. Dong, "Novel secure communication based on chaos synchronization," *IEICE Transactions on Fundamentals of Electronics, Communications and Computer Sciences*, vol. 101, no. 7, pp. 1132–1135, 2018.

[37] S. Bendoukha, S. Abdelmalek, and A. Ouannas, "Secure communication systems based on the synchronization of chaotic systems," in *Mathematics Applied to Engineering, Modelling, and Social Issues*, vol. 20, pp. 281–311, Springer, Cham, Switzerland, 2019.

[38] K. M. Cuomo and A. V. Oppenheim, "Circuit implementation of synchronized chaos with applications to communications," *Physical Review Letters*, vol. 71, no. 1, pp. 65–68, 1993.

[39] J. Chen, C. Li, and X. Yang, "Chaos synchronization of the distributed-order Lorenz system via active control and applications in chaotic masking," *International Journal of Bifurcation and Chaos*, vol. 28, no. 10, Article ID 1850121, 2018.

[40] T. Yang and L. O. Chua, "Secure communication via chaotic parameter modulation," *IEEE Transactions on Circuits and Systems I: Fundamental Theory and Applications*, vol. 43, no. 9, pp. 817–819, 1996.

[41] G. Cheng, L. Wang, Q. Chen, and G. Chen, "Design and performance analysis of generalised carrier index M-ary differential chaos shift keying modulation," *IET Communications*, vol. 12, no. 11, pp. 1324–1331, 2018.

[42] U. Feldmann, M. Hasler, and W. Schwarz, "Communication by chaotic signals: the inverse system approach," in *Proceedings of the 1995 IEEE International Symposium on Circuits and Systems-ISCAS 95. Part 3 (of 3)*, vol. 1, pp. 680–683, IEEE, May 1995.

[43] S. Hayes, C. Grebogi, and E. Ott, "Communicating with chaos," *Physical Review Letters*, vol. 70, no. 20, pp. 3031–3034, 1993.

[44] E. Tlelo-Cuautle, O. Guilln-Fernndez, J. Rangel-Magdaleno et al., "FPGA implementation of chaotic oscillators, their synchronization, and application to secure communications," in *Recent Advances in Chaotic Systems and Synchronization*, pp. 301–328, Academic Press, 2019.

[45] S. He, K. Sun, H. Wang, X. Mei, and Y. Sun, "Generalized synchronization of fractional-order hyperchaotic systems and its DSP implementation," *Nonlinear Dynamics*, vol. 92, no. 1, pp. 85–96, 2018.

[46] D. Peng, K. H. Sun, and A. O. Alamodi, "Dynamics analysis of fractional-order permanent magnet synchronous motor and its DSP implementation," *International Journal of Modern Physics B*, vol. 33, no. 6, Article ID 1950031, 2019.

[47] Z. Li and D. Xu, "A secure communication scheme using projective chaos synchronization," *Chaos, Solitons & Fractals*, vol. 22, no. 2, pp. 477–481, 2004.

[48] M. Feki, "An adaptive chaos synchronization scheme applied to secure communication," *Chaos, Solitons & Fractals*, vol. 18, no. 1, pp. 141–148, 2003.

[49] T. Kapitaniak and W.-H. Steeb, "Transition to hyperchaos in coupled generalized van der Pol equations," *Physics Letters A*, vol. 152, no. 1-2, pp. 33–36, 1991.

[50] H. Richter, "The generalized Henon maps: examples for higher-dimensional chaos," *International Journal of Bifurcation and Chaos*, vol. 12, no. 6, pp. 1371–1384, 2002.

[51] K. Geist, U. Parlitz, and W. Lauterborn, "Comparison of different methods for computing Lyapunov exponents," *Progress of Theoretical and Experimental Physics*, vol. 83, no. 5, pp. 875–893, 1990.

[52] S. H. Strogatz, *Nonlinear Dynamics And Chaos with Applications to Physics, Biology, Chemistry, and Engineering*, CRC Press, 2018.

[53] W. Gao, Y. Wang, and A. Homaifa, "Discrete-time variable structure control systems," *IEEE Transactions on Industrial Electronics*, vol. 42, no. 2, pp. 117–122, 1995.

[54] Y.-X. Zhao, T. Wu, and Y. Ma, "A double power reaching law of sliding mode control based on neural network," *Mathematical Problems in Engineering*, vol. 2013, Article ID 408272, 9 pages, 2013.